Final Technical Report

Unimolecular Reaction Dynamics of Free Radicals

(DE-FG02-02ER15284)

Terry A. Miller
Department of Chemistry, The Ohio State University
Columbus OH 43210-1106, email: miller.104@osu.edu

1 Program Scope

Radical reactions are of crucial importance in combustion and in atmospheric chemistry. Reliable theoretical models for predicting the rates and products of these reactions are required for modeling combustion and atmospheric chemistry systems. Modern computer codes employed to simulate combustion or atmospheric chemistry include several hundreds of radical reactions. Among them unimolecular reactions frequently play a crucial role in determining final products. The branching ratios in bimolecular reactions that proceed via complex formation and unimolecular dissociation are an important class. In contrast to the unimolecular reactions of stable molecules such as the benchmark reaction, $CH_2CO \rightarrow {}^{1,3}CH_2 + CO$, the reactions of free radicals occur over energy barriers sufficiently low that the hypothesis of rapid energy randomization upon which statistical transition state theories depend is in doubt.

The dissociations of vinyl, CH_2= CH, and methoxy, CH_3O, have low barriers, about 13,000 cm^{-1} and 8,000 cm^{-1}, respectively. As for many other free radicals, the low barrier for dissociation results from the simultaneous increase in the bond order of C-C and C-O in vinyl and methoxy radicals respectively as the C-H bond is broken. These reactions should serve as benchmarks for this important class of reactions. The ultimate goal of this work is a quantitative understanding of the unimolecular reactions dynamics of free radicals. To achieve this goal, a detailed understanding of the vinyl and methoxy radicals is required

2 Accomplishments

Work on the vinyl radical concentrated on the dynamics of dissociation of vinyl and d_2-vinyl radicals in the range of high excitation energies of their $\tilde{X}$ states: E ≈ 6750 – 9150 cm^{-1} above the dissociation barrier.

2.1 Vinyl radical

The energy interval E ≈ 6750 – 9150 cm^{-1} can be accessible via excitation of vinyl radical to the $\tilde{A}$ state. The rovibrational structure of the $\tilde{A}$ state was extensively investigated in our early DOE supported work. Excitation of vinyl radical to the $\tilde{A}$ state leads to the dissociation of vinyl radical via internal conversion into highly excited vibrational levels of the $\tilde{X}$ state. This was used as the

method of energy deposition above the dissociation barrier of the $\tilde{X}$ state. Velocity maps of H and D atoms that are products of CH_2=CH and CD_2=CH dissociation accompanied by acetylene, were measured in the excitation energy range E ≈ 6750 – 9150 cm^{-1} above the dissociation barrier of the $\tilde{X}$ state. Rovibrational energy dependencies on the excitation energy, E, inferred for acetylene and d_1-acetylene products are compared with theoretically predicted ones. An upper bound is derived for the rate constant of H-atom scrambling between the α- and β-carbon atoms.

Velocity map measurements of H and D atoms that are products of CH_2= CH and CD_2=CH dissociation, were accomplished in the excitation energy range of 8200 – 10600 cm^{-1} above products zero point energy. As pointed out above, this corresponds to approximately 6750 – 9150 cm^{-1} energy above the dissociation barrier in the $\tilde{X}$ state. We were able to measure velocity distributions of the H product of reaction (1) as well as the D product of the reaction (1'),

$$CH_2{=}CH \rightarrow CH{\equiv}CH + H \qquad (1)$$

$$CD_2 = CH \rightarrow CD \equiv CH + D \qquad (1')$$

for six vibrational bands of C_2H_3 and for seven bands of CD_2CH of the $\tilde{A}$ state. Two-dimensional (2-D) velocity maps of H and D atoms that are products of CH_2=CH and CD_2=CH dissociation, respectively, were recorded.

A typical H-atom raw 2-D image from vinyl radical excitation to the 6^2, 6^18^1 bands of the $\tilde{A}$ state is shown in Fig. 1(a). In Fig.1 (b) the Abel inverse transformed image is shown.

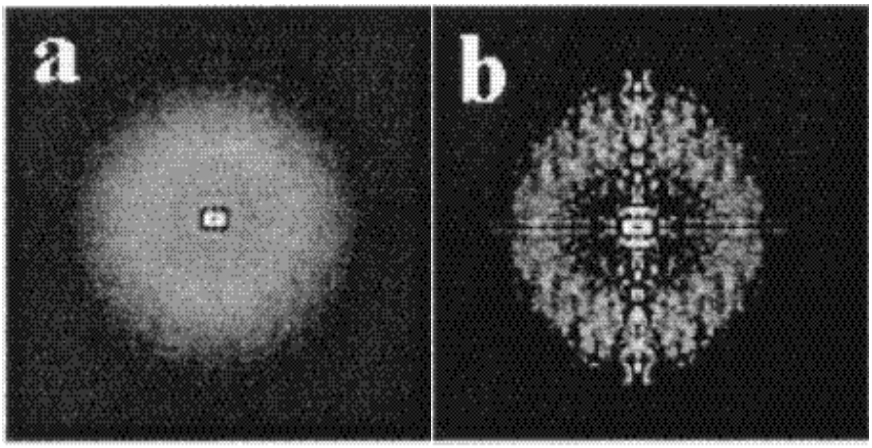

Fig.1. Typical H-atom images from vinyl radical excitation to the 6^2, 6^18^1 bands at 22 391 cm^{-1}.
(a) Raw image;
(b) Reconstructed image.

Figs. 2 and Fig. 3 show the H-atom speed distribution and anisotropy parameter extracted from the image data in Fig. 1. These data were obtained for all vibrational bands and gave important dynamical characteristics of unimolecular dissociation of the vinyl radical in its ground $\tilde{X}\,^2A'$ electronic state. The distributions of translational and total internal (E_{int}=E_{vib} + E_{rot}) energy of acetylene and d_1- acetylene products in the excitation energy range 6750 – 9150 cm^{-1} above the dissociation barrier are determined from the H-atom speed distributions by simple conservation of energy and compared with theoretically predicted ones. It was found, as expected, that these distributions are statistical.

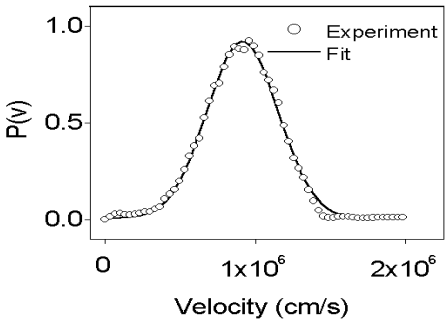

Fig. 2. H atoms speed distribution P(*v*) from image data in Fig. 1.

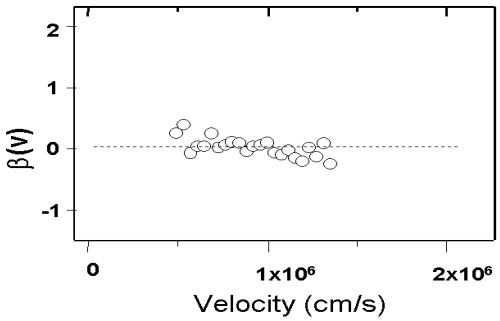

Fig. 3. H atoms anisotropy parameters β(*v)* extracted at selected velocities from image data in Fig. 1.

The possibility of significant H-atom scrambling:

$$CD_2 = CH \rightarrow CHD = CD \qquad (2),$$

followed by dissociation

$$CHD = CD \rightarrow CD \equiv CD + H \quad (1''),$$

is ruled out by the experimental data shown in Fig. 4. In this figure, REMPI spectra of both H and D atoms are shown. Each spectrum consists of two traces - one with and one - without the laser that dissociates CD_2CH. Left traces show little or no difference, reflecting the lack of H-atom products from d_2-vinyl excitation. The D-atom profiles on the right part of Fig. 4 clearly show the "cold" D atoms entrained in the molecular beam, and the additional translationally "hot" D atoms produced after vinyl excitation. These facts, reflected in Fig. 4, allow an upper bound of 1.3×10^{11} s^{-1} to be derived for the rate constant of H-atom scrambling between the α and β carbon atoms.

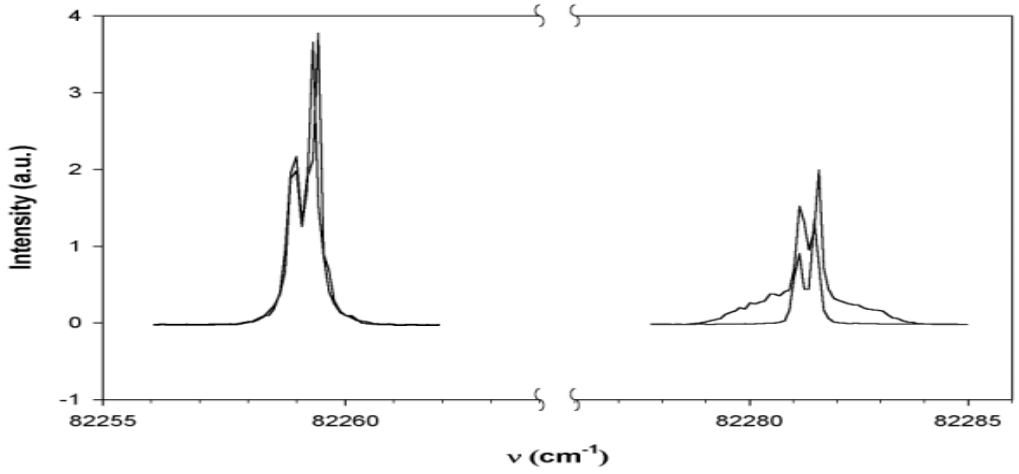

Fig. 4. REMPI spectra of H and D from excitation to the 5^2 band of CD_2CH at 22330 cm^{-1}. Both consist of two traces taken with and without the excitation laser. The H atom profiles on the left show little or no difference on this scale, reflecting the lack of H atom product from vinyl excitation. The D atom profiles on the right clearly show the "cold" D atom entrained in the molecular beam (excitation laser "OFF"), and the additional "hot" D atoms produced with excitation laser "ON".

2.2 Methoxy

As mentioned in the Introduction methoxy has a low barrier for dissociation into formaldehyde and H atom. The schematic potential diagram is shown in Fig. 5. By performing the pump/dump experiment illustrated in Fig. 5 specific highly excited vibrational states of methoxy may be prepared with energies near the barrier. Studies, e.g., via H detection, of dissociation from such levels would be a sensitive test of how statistical the dynamics truly are.

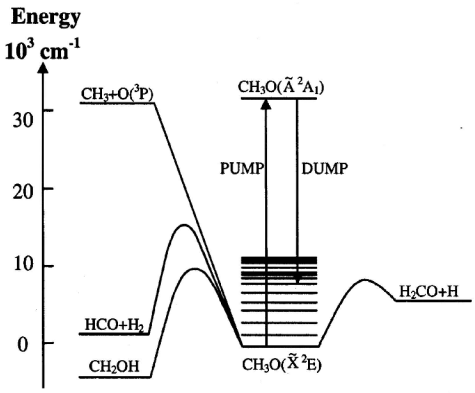

Fig. 5. Schematic potential diagram for $CH_3O(\tilde{X}^2E)$ and $CH_3O(\tilde{A}^2A_1)$ with illustration of SEP scheme for the preparation of specific highly excited states of $CH_3O(\tilde{X})$.

However, the interpretation, indeed even the design, of such dynamical experiments requires detailed understanding of the spectroscopy of the methoxy radical. Such understanding

must include spin-vibronic assignments. With CH_3O, it has previously been shown that "reading the rotational bar code" of a given spin-vibronic level may be the surest means of its assignment. Hence the analysis of the rotational structure of a number of methoxy bands is also critical.

Additionally, the spectroscopy of CH_3O is known to be complicated by the degeneracy of its ground electronic state (X^2E) and its asymmetric (e) vibrational modes. The Jahn-Teller effect vibronically couples the methoxy electronic and vibrational levels to remove some of the degeneracy but with a very complicated vibronic energy level pattern resulting. In principle, partial deuteration to give CHD_2O transforms the Jahn-Teller effect into a pseudo-Jahn-Teller effect and produces a single non-degenerate C-H stretch vibration from the previous 3 C-H stretch motions (a_1 ν_1 and e ν_4). Hence the spectroscopy and ultimately the dynamics of CHD_2O are of great interest. Moreover while not as interesting dynamically, the isotopomer CH_2DO, may be critical to the spectroscopic understanding of CHD_2O.

Extensive efforts have been made to obtain a variety of spectroscopic data for methoxy including laser induced fluorescence (LIF), laser excited dispersed fluorescence (LEDF), fluorescence dip infrared (FDIR) and stimulated emission pumping (SEP). Table 1 lists the vibrational bands for the $\tilde{A}^2A$ - $\tilde{X}^2E$ electronic transition for which we presently have data. Examples of typical LEDF, FDIR, and SEP spectra are shown in Fig. 6.

Analyses of the spectra listed in Table 1 are on-going. A detailed rotational analysis of several bands of CHD_2O is almost complete. This will constitute the first such analysis of an asymmetrically substituted methoxy radical. Additionally work involving the assignment of numerous higher energy vibronic bands in both CH_3O and CHD_2O is progressing. Such results are critical for implementing dynamics experiments near the dissociation barrier.

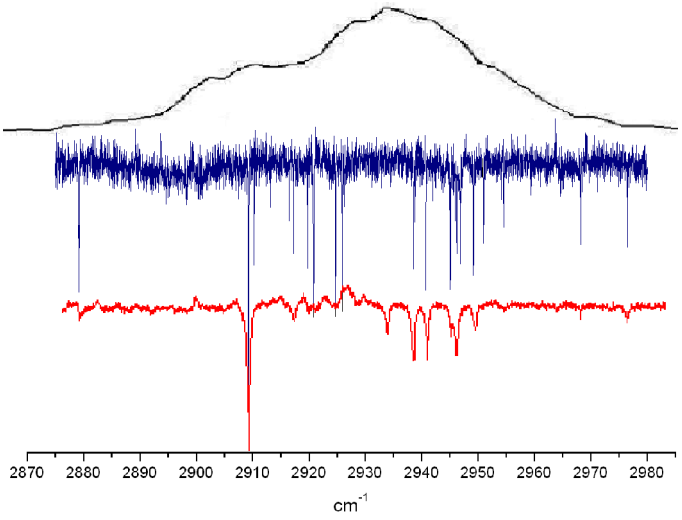

Fig. 6. Three separate traces of C-H stretch region in CH_3O. Top trace is an LEDF spectrum with $3^1 4^1$ band in $\tilde{A}^2A$ state pumped. Middle trace is an FDIR spectrum. Bottom trace is SEP spectrum through the excitation of |N=1, K=0> rotational line of 3^5 band in $\tilde{A}^2A$ state.

Table 1
Summary of vibrational bands for which spectroscopic data for CH_3O and CHD_2O have been obtained in these studies

	LIF	LEDF	SEP
CH_3O	$3^1 4^1$ $3^2 4^1$ $3^3 4^1$ 3^5	$3^1 4^1, 3^2 4^1$ $3^3 4^1, 3^5, 3^3 5^1$ $3^3 6^1, 3^2 6^2$(a), $3^2 6^2$(e)	$3^1 4^1$ $3^2 4^1$ 3^5
CHD_2O	$0^0, 3^1 1^1, (5')^1, (6')^1$ $(6'')^1, 3^2 1^1, 3^5, 3^2 (4^1)^1, (5'')^1$	$3^1 1^1$ $3^2 1^1$ 3^5 $3^2 (5')^1$ $3^2 (5'')^1$ $3^2 (6')^1$ $3^2 (6'')^1$	0^{0b} $3^1 1^1$ $(5')^1$ $(6')^1$ $(6'')^1$ $3^2 1^1$ 3^5

[a]The vibrational numbering is standard for CH_3O. For CHD_2O, the C_{3v} degenerate e vibrations are resolved in C_{2v} symmetry into corresponding a′ and a″ components which are denoted in the table by one of two primes respectively.

[b]Transition to $\tilde{X}^2 E_{1/2}$.